Computer Assisted Mechanics and Engineering Sciences, 6: 231–244, 1999.

Material modelling for structures subjected to impulsive loading

Krzysztof Cichocki, Robert Adamczyk and Mariusz Ruchwa
Technical University of Koszalin, Racławicka 15–17, 75-620 Koszalin, Poland

(Received July 24, 1998)

The main results of numerical analyses of a possible design configuration of a submerged structure subjected to impulsive loading due to explosion, performed for various material models assumed for a plain concrete are presented and discussed. Three different models were considered — the modified Drucker–Prager plasticity model, brittle cracking model and the elastoplastic model with damage. The present study suggests problems and possible solutions to be applied into numerical analysis of such structures by means of available finite element computer codes.

1. Introduction

The ability of sandwich structures to absorb energy under impulsive loading conditions is the main reason of their utilisation in situations when the structure has to protected against such kind of loads. In typical engineering situations, mostly concerning so-called "lifelines" as pipelines, underwater tunnel crossings, the designer requires reliable prediction of the most severe consequences of impulsive loading (impacts, explosions) in terms of permanent deflections, damaged zones in structures, as well as cracking, spalling and loss of overall structural integrity.

In order to evaluate these effects and their influence on the structural load-carrying ability, the numerical simulation of above mentioned phenomena are often performed, using the professional general-purpose computer codes. General studies have been published recently, covered in recent revievs [2, 3, 6–9, 14, 15, 18, 19].

Among many problems to be solved building the discrete model, the fundamental importance has the assumed material model. Due to the fact of highly nonlinear, rate-dependent behaviour of the typical structural materials, such as ductile steel and plain concrete, the constitutive material models adopted in analysis are relatively complex and difficult to implement into finite element computer code. Many comments and considerations concerning various aspects of the numerical simulations of such phenomena were presented by Cichocki *et al.* [6, 8, 9].

The purpose of the present paper is to compare the results of numerical simulation of the dynamic response of underwater structure to explosion performed for various material models assumed for concrete. The structure under consideration is the underwater buoyant tunnel, intended for a railway crossing of strait or channel. The tunnel basically is a cylindrical shell with horizontal axis, circular cross section and 15 m external diameter. Detailed description of its geometry and structural configuration of elements is published in [8]. A portion of the structural system in point is presented in the Fig. 1. The schematic view of the entire cylindrical structure (Fig. 1a) shows also the location of explosive charge (point X). The details of the structure are visible in Fig. 1b, where the finite element mesh adopted for a numerical analysis is presented. The internal sandwich cylinder (25 mm steel – 450 mm plain concrete – 25 mm steel) is connected with external protective structure, realised as the 32 mm thick steel cylindrical shell. The circumferential stiffeners ensure the rigidity of the protective structure. Externally the structure is covered by 10 cm thick concrete layer.

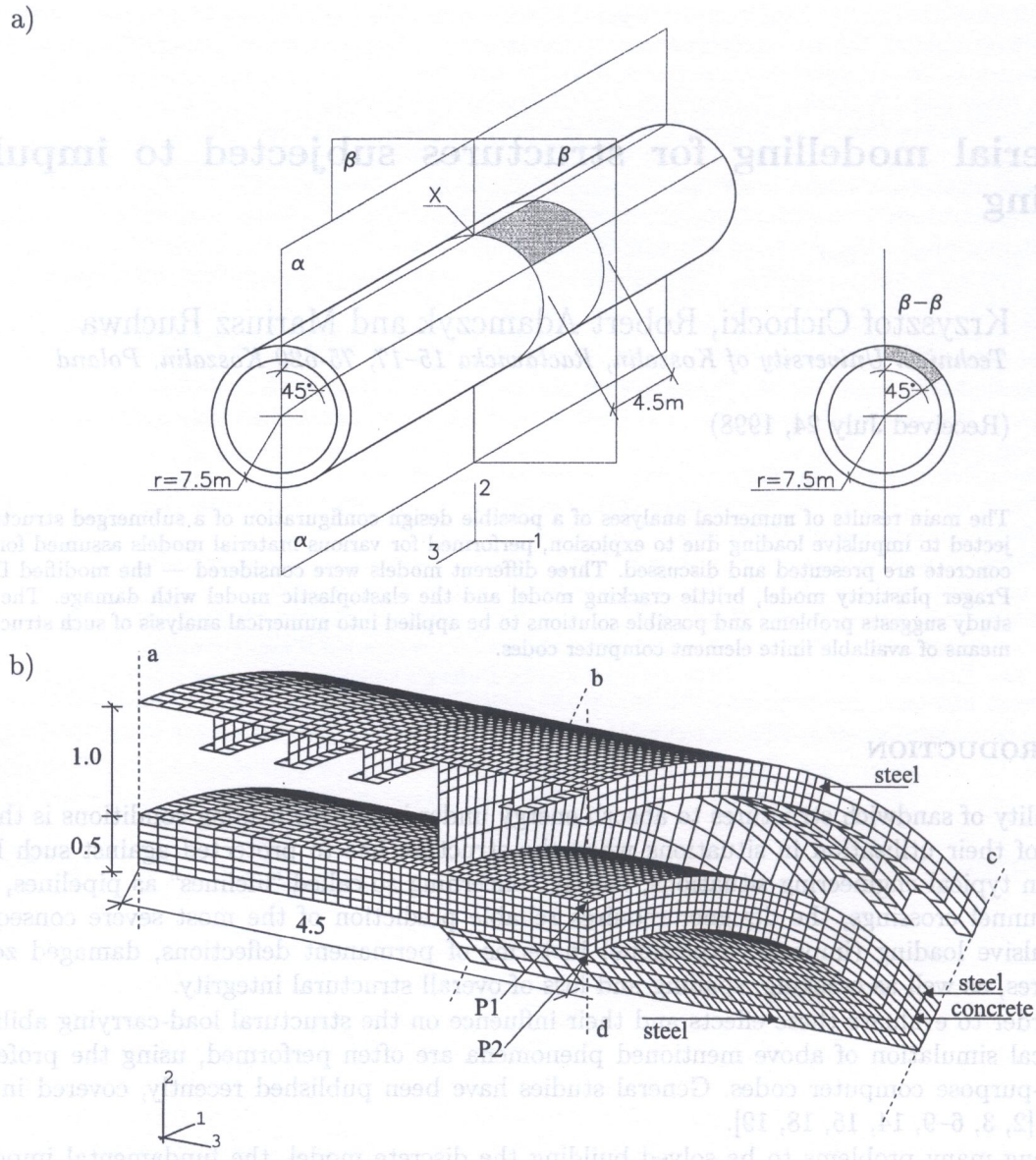

Fig. 1. Tunnel. a) schematic view of structure (X – explosive charge), b) view of entire mesh. Boundary conditions: plane surfaces a–b, b–c: fixed nodes; plane surfaces c–d, a–d: symmetry

On the basis of preliminary considerations, the 40 kg spherical charge of trinitrotoluene (TNT) placed on the external surface of the protective containment was taken into account as the representative case of impulsive load. The load produced during an underwater explosion was modelled as the known field of pressure, variable in time and space. The description of pressure was obtained on the basis of semiempirical equations proposed by Henrych [12], and modified in order to capture the reflection phenomena on the curved surface of the external cylinder (Srivastava [20]). To check the validity of the implemented algorithm several numerical tests were performed. The whole (water–explosive charge–cylindrical structure) system was discretized using Jones–Wilkens–Lee and Mie–Gruneisen equations of state for explosive charge and water [1]. The obtained results, published in [2], present a good approximation of the pressure field calculated by the implemented Henrych's formulation.

All analyses were realised using the ABAQUS/Explicit computer code in version 5.7 [1], together with adequate subroutines written by authors, which give the load description according the adopted Henrych's formula, and the assumed constitutive material models considered below.

2. MATERIAL MODELS

2.1. Elastoplastic model for steel

In the entire analysis, an unique constitutive model was assumed for steel according to von Mises yielding criterion with isotropic hardening, softening and associated flow rule. Rate-dependent behaviour of steel was captured by well-known Cowper–Symonds model [5]. In uniaxial variables this model is defined by the following equation, expressing the rate-dependent hardening curves in terms of the static relation [13, 21]

$$\sigma(\varepsilon^{\mathrm{p}}_{\mathrm{eq}}\,,\,\dot{\varepsilon}^{\mathrm{p}}_{\mathrm{eq}}) = \sigma^{0}(\varepsilon^{\mathrm{p}}_{\mathrm{eq}})\,R(\dot{\varepsilon}^{\mathrm{p}}_{\mathrm{eq}}) \tag{1}$$

where σ^0 is the static yield stress, $\varepsilon^{\mathrm{p}}_{\mathrm{eq}}$ is the equivalent plastic strain, $\dot{\varepsilon}^{\mathrm{p}}_{\mathrm{eq}}$ is the equivalent plastic strain rate, and R is the ratio of the yield stress at non-zero strain rate to the static yield stress ($R = 1$ for $\dot{\varepsilon}^{\mathrm{p}}_{\mathrm{eq}} = 0$). Ratio R was defined by the overstress power law, having the following form:

$$R = \left(\frac{\dot{\varepsilon}^{\mathrm{p}}_{\mathrm{eq}}}{m}\right)^{\frac{1}{n}} + 1 \tag{2}$$

where m, n are two material parameters (for ductile steel $m = 40\,\mathrm{s}^{-1}$, $n = 5$ [13]).

To model the damage of material the ductile failure formulation was assumed, based on the maximum values of plastic equivalent strain $\varepsilon^{\mathrm{p}}_{\mathrm{eq}}$ defined as follows:

$$\varepsilon^{\mathrm{p}}_{\mathrm{eq}} = \int_0^t \sqrt{\frac{2}{3}\,(\dot{\boldsymbol{\varepsilon}}^{\mathrm{p}} : \dot{\boldsymbol{\varepsilon}}^{\mathrm{p}})}\,\mathrm{d}t \tag{3}$$

where $\dot{\boldsymbol{\varepsilon}}^{\mathrm{p}}$ is the plastic strain rate tensor. In this model, the damage D can be calculated as below:

$$D = \frac{\varepsilon^{\mathrm{p}}_{\mathrm{eq}} - \varepsilon^{\mathrm{p}}_{\mathrm{eq},0}}{\varepsilon^{\mathrm{p}}_{\mathrm{eq},f} - \varepsilon^{\mathrm{p}}_{\mathrm{eq},0}} \tag{4}$$

where $\varepsilon^{\mathrm{p}}_{\mathrm{eq}}$ is the current equivalent plastic strain, $\varepsilon^{\mathrm{p}}_{\mathrm{eq},0}$, $\varepsilon^{\mathrm{p}}_{\mathrm{eq},f}$ denote the initial and final value of equivalent plastic strain, i.e. when the damage phenomenon starts ($D = 0$) and finishes ($D = 1$).

Due to this formulation, the elastic response is simply based on damaged elasticity. The damaged elastic moduli (G_D – shear modulus, K_D – bulk modulus) are defined by:

$$G_D = (1 - D)G\,, \qquad K_D = (1 - D)K\,. \tag{5}$$

The damaged plastic yield surface also depends on the value D:

$$\sigma_{\mathrm{yd}} = (1 - D)\,\sigma_{\mathrm{y}}(\varepsilon^{\mathrm{p}}_{\mathrm{eq}}). \tag{6}$$

The set of material characteristics assumed for the analysis is given in Table 1.

Table 1. Material characteristics for steel

yield stress	345 MPa
strength in compression	700 MPa
plastic strain corresponding the strength	0.20
equivalent plastic strain $\varepsilon^{\mathrm{p}}_{\mathrm{eq},0}$	0.25
equivalent plastic strain $\varepsilon^{\mathrm{p}}_{\mathrm{eq},f}$	0.45

2.2. Modified Drucker–Prager model for concrete

The modified Drucker–Prager model is defined by the yield surface, expressed in terms of deviatoric stresses

$$F_s = t - p\tan\beta - d \tag{7}$$

where t is the deviatoric stress $\mathbf{s}$ measure, p is the equivalent pressure stress,

$$t = \frac{q}{2}\left[1 + \frac{1}{\kappa} - \left(1 - \frac{1}{\kappa}\right)\left(\frac{r}{q}\right)^3\right],$$
$$p = -\frac{1}{3}\operatorname{trace}(\boldsymbol{\sigma}), \qquad q = \sqrt{\frac{3}{2}(\mathbf{s}:\mathbf{s})}, \qquad r = \left(\frac{9}{2}\mathbf{s}\cdot\mathbf{s}:\mathbf{s}\right)^{\frac{1}{3}}, \tag{8}$$

κ is a material parameter which gives the dependence on the third deviatoric stress invariant (for $\kappa = 1$ this dependence is cancelled, and the yield surface has a circular cross section in the deviatoric plane). Parameter β is the material's angle of friction, d is the cohesion.

The yield surface is completed by the cap of an elliptical shape with constant eccentricity in the p–t plane, expressed as follows:

$$F_c = \sqrt{(p - p_\mathrm{a})^2 + \left(\frac{Rt}{1 + \alpha - \alpha/\cos\beta}\right)^2} - R(d + p_\mathrm{a}\tan\beta) = 0 \tag{9}$$

where R is a material parameter, α is a parameter which gives the smooth transition between yield surface (7) and the cap (9). Parameter p_a defines the hardening/softening of the cap, depending on the volumetric plastic strain:

$$p_\mathrm{a} = \frac{p_\mathrm{b} - Rd}{1 + R\tan\beta} \tag{10}$$

where p_b is the hydrostatic compression yield stress.

The model is completed by the flow rule, according to flow potential surfaces defined in [1, 11].

In order to obtain the proper values of parameters defining the model, several tests have been performed on the basis of experimental results presented in [4, 22, 23]. The basic values applied in further analysis are listed in Table 2.

Table 2. Parameters of modified Drucker–Prager model for concrete

material cohesion d	6.14 MPa
material angle of friction β	60°
cap eccentricity parameter R	0.11
volumetric plastic strain $\varepsilon_\mathrm{v}^\mathrm{p}$ for the initial cap yield surface position	0.0
transition surface radius parameter α	0.01

2.3. Brittle cracking model for concrete

The cracking model adopted in ABAQUS/Explicit serves to model the brittle cracking behaviour of plain concrete, with the assumption of linear elastic characteristics in compression. In this approach the smeared crack assumption has been made together with fixed orthogonal crack directions. To detect the crack initiation a simple Rankine criterion is applied — a crack starts to form when the maximum principal tensile stress exceeds the tensile strength of material. The crack surface is

assumed to be normal to the direction of the maximum tensile principal stress. The consequent closing and reopening of the crack is also possible.

Analogically to the yield conditions in classical plasticity, a consistency condition for cracking was introduced in a form of tensor:

$$\mathbf{C} = \mathbf{C}\left(\mathbf{t}, \boldsymbol{\sigma}^{\mathrm{I,II}}\right) = \mathbf{0} \tag{11}$$

where $\mathbf{C} = [C_{nn}, C_{tt}, C_{ss}, C_{nt}, C_{ns}, C_{ts}]^{\mathrm{T}}$ is a tensor written in the crack direction coordinate system, and $\boldsymbol{\sigma}^{\mathrm{I,II}}$ represents a tension softening model in the case of the direct components of stress and a shear softening/retention model in the case of the shear components of stress. The stress quantities $\mathbf{t} = [t_{nn}, t_{tt}, t_{ss}, t_{nt}, t_{ns}, t_{ts}]^{\mathrm{T}}$ are expressed in the local "cracking" system.

The cracking condition for particular crack normal direction n can be written explicitly:

$$C_{nn} = C_{nn}(t_{nn}, \sigma_t^{\mathrm{I}}) = t_{nn} - \sigma_t^{\mathrm{I}}(e_{nn}^{\mathrm{ck}}) = 0 \tag{12}$$

where e_{nn}^{ck} is the adequate value of strain in the local n direction and $\sigma_t^{\mathrm{I}}(e_{nn}^{\mathrm{ck}})$ is the tension softening evolution.

For the closing/reopening crack, the adequate condition has the following form:

$$C_{nn} = C_{nn}(t_{nn}, \sigma_c^{\mathrm{I}}) = t_{nn} - \sigma_c^{\mathrm{I}}(e_{nn}^{\mathrm{ck}})\Big|_{e_{nn}^{\mathrm{open}}} = 0 \tag{13}$$

In this case, the value of $\sigma_c^{\mathrm{I}}(e_{nn}^{\mathrm{ck}})|_{e_{nn}^{\mathrm{open}}}$ is the crack closing/reopening evolution. Maximum crack opening strain is defined as

$$e_{nn}^{\mathrm{open}} = \max(e_{nn}^{\mathrm{ck}})$$

measured over history. Similar conditions could be written for directions t and s.

The shear cracking condition for component nt can be expressed as follows:

$$C_{nt} = C_{nt}(t_{nt}, \sigma_s^{\mathrm{II}}) = t_{nt} - \sigma_s^{\mathrm{II}}(g_{nt}^{\mathrm{ck}}, e_{nn}^{\mathrm{ck}}, e_{tt}^{\mathrm{ck}}) = 0 \tag{14}$$

where $\sigma_s^{\mathrm{II}}(g_{nt}^{\mathrm{ck}}, e_{nn}^{\mathrm{ck}}, e_{tt}^{\mathrm{ck}})$ is the evolution of shear, depending linearly on the shear strain, and also on the crack opening strain. The adequate conditions for components ns and ts have the similar form.

This brittle cracking constitutive model is available in ABAQUS/Explicit ver. 5.7 [1], and has been used to model the behaviour of concrete in a core of internal sandwich structure. Assumed parameters of this model are listed in Table 3.

Table 3. Parameters of brittle cracking model for concrete

remaining direct stress after cracking σ_t^{I}	direct cracking strain e_{nn}^{ck}
10 MPa	0.0
0.1 MPa	0.005
shear retention factor ρ according to [1]	crack opening strain e_{nn}^{ck}
1.0	0.0
0.01	0.05

2.4. Elastoplastic damage model for concrete

In order to include a damage into the constitutive models for concrete, an alternative model has been developed on the basis of considerations presented by Comi *et al.* [10]. This elastoplastic damage model is intended to model the behaviour up to rupture of so-called ductile–brittle materials, particularly under compressive loading. The macroscopic effects of the microscopic degradation of the material can be modelled by a single scalar damage variable, denoted by D [16, 17].

The Helmholtz specific free energy Ψ is a function of the damage variable D and of elastic strain tensor $\boldsymbol{\varepsilon}^{\mathrm{e}} = \boldsymbol{\varepsilon} - \boldsymbol{\varepsilon}^{\mathrm{in}}$, where $\boldsymbol{\varepsilon}^{\mathrm{in}}$ is an inelastic strain tensor. The stress tensor can be derived from the following expression (ρ is the material density):

$$\boldsymbol{\sigma} = \rho \frac{\partial \Psi}{\partial \boldsymbol{\varepsilon}} = -\rho \frac{\partial \Psi}{\partial \boldsymbol{\varepsilon}^{\mathrm{in}}} . \tag{15}$$

For the free energy, the following form was assumed:

$$\rho\Psi = \frac{1}{2}(1-D)\left[K\left(\varepsilon_{\mathrm{v}} - \varepsilon_{\mathrm{v}}^{\mathrm{in}}\right)^2 + 2G(1-aD)\left(\mathbf{e}-\mathbf{e}^{\mathrm{in}}\right):\left(\mathbf{e}-\mathbf{e}^{\mathrm{in}}\right)\right] \tag{16}$$

where G and K are respectively shear and bulk moduli of the undamaged material, ε_{v} is the volumetric and $\mathbf{e}$ is the deviatoric part of the strain tensor $\boldsymbol{\varepsilon}$. Parameter a gives the different dependence on D for "damaged" moduli G_D, K_D [10]:

$$G_D = (1-D)(1-aD)G\,, \qquad K_D = (1-D)K\,. \tag{17}$$

The assumption of free energy Ψ gives the following expression for stress tensor $\boldsymbol{\sigma}$ and damage strain energy release rate Y:

$$\begin{aligned} \boldsymbol{\sigma} &= (1-D)\left[K\left(\varepsilon_{\mathrm{v}} - \varepsilon_{\mathrm{v}}^{\mathrm{in}}\right)\mathbf{1} + 2G(1-aD)\left(\mathbf{e}-\mathbf{e}^{\mathrm{in}}\right):\left(\mathbf{e}-\mathbf{e}^{\mathrm{in}}\right)\right], \\ Y &= \frac{1}{2}\left[K\left(\varepsilon_{\mathrm{v}} - \varepsilon_{\mathrm{v}}^{\mathrm{in}}\right)^2 + 2G(1+a-2aD)\left(\mathbf{e}-\mathbf{e}^{\mathrm{in}}\right):\left(\mathbf{e}-\mathbf{e}^{\mathrm{in}}\right)\right]. \end{aligned} \tag{18}$$

The yield function, defining the elastic domain is defined by the expression

$$f(\boldsymbol{\sigma}; D) = \frac{I_1^2}{18K(1-D)^2} + \frac{J_2^2}{2G(1-D)^2(1-aD)} + \frac{b_1(1+b_2D)}{1-D} I_1 - R \tag{19}$$

where

$I1 = \mathrm{Tr}(\boldsymbol{\sigma})$ – first invariant of stress tensor $\boldsymbol{\sigma}$

$J_2 = \frac{1}{2}\mathbf{s} : \mathbf{s}$ – second invariant of stress deviator $\mathbf{s}$

$R = b_3 D + b_4$

b_i – material dependent parameters

The yielding criterion is completed by a tension cut-off:

$$I_1 - r(D) \leq 0. \tag{20}$$

The evolution of the hardening function R is governed by damage D. For total degradation of the material $D = 1$.

To complete the constitutive model presented here, the expression for inelastic potential $g(\boldsymbol{\sigma}, Y; D)$ was obtained, where:

$$\begin{aligned} Y &= -\rho \frac{\partial \Psi}{\partial D}\,, \\ g &= g_{\mathrm{in}}(\boldsymbol{\sigma}; D) + g_{\mathrm{d}}(Y; D), \\ g_{\mathrm{in}}(\boldsymbol{\sigma}; D) &= \frac{b_7}{18K} I_1^2 + \frac{b_6}{2G(1-aD)} J_2 + b_8(1+b_2D)(1-D)I_1\,, \\ g_{\mathrm{d}}(Y; D) &= Y\,. \end{aligned} \tag{21}$$

On this basis it is possible to define the rate of inelastic strain tensor $\dot{\boldsymbol{\varepsilon}}^{\text{in}}$ and damage $\dot{D}$:

$$\begin{aligned} \dot{\boldsymbol{\varepsilon}} &= \dot{\lambda}\frac{\partial g}{\partial \boldsymbol{\sigma}} = \dot{\lambda}\left\{\left[\frac{b_7}{9K}I_1^2 + b_8(1+b_2D)(1-D)\right]\mathbf{1} + \frac{b_6}{2G(1-aD)}\mathbf{s}\right\}, \\ \dot{D} &= \dot{\lambda}, \end{aligned} \tag{22}$$

where $\dot{\lambda}$ is the plastic multiplier [16].

The constitutive model based on the above made assumptions has been implemented into the algorithm of an explicit (central difference method) integration in a time domain, as user's subroutine VUMAT in ABAQUS/Explicit computer code.

Table 4. Parameters of elastoplastic model with damage for concrete

b_1	$550 \cdot 10^{-6}$
b_2	5.5
b_3	0.02 MPa
b_4	0.002 MPa
b_6	1.47
b_7	1.02
b_8	$550 \cdot 10^{-6}$

3. Discussion of results

Three independent analyses have been performed, each for another material model for concrete. In order to compare the obtained results, several fundamental quantities have been examined for all three cases. First of all, the value of total energy dissipated in plastic effects was calculated and presented in Fig. 2. The shapes of a curve indicate that for entire structure all the dissipative effects practically vanish after approximately 12 milliseconds after the explosion. The major part of energy was dissipated by the external protective structure. The small differences in final values are due to different material formulations; the highest value is for Drucker–Prager model, the lowest value is for the brittle cracking formulation, where there is no plastic flow at all. The elastoplastic model with damage gives the intermediate value.

Figure 3 shows the final deformed shapes of the mesh. Damaged elements of the external protective shell were cancelled from the mesh. Additionally, in Fig. 3c, the damaged elements of concrete

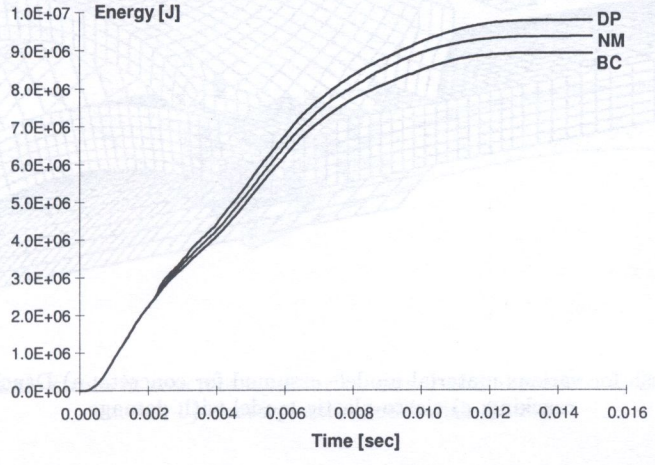

Fig. 2. Energy dissipated by plastic deformation for various material models assumed for concrete. (DP: Drucker–Prager, BC: brittle cracking, NM: elastoplastic model with damage)

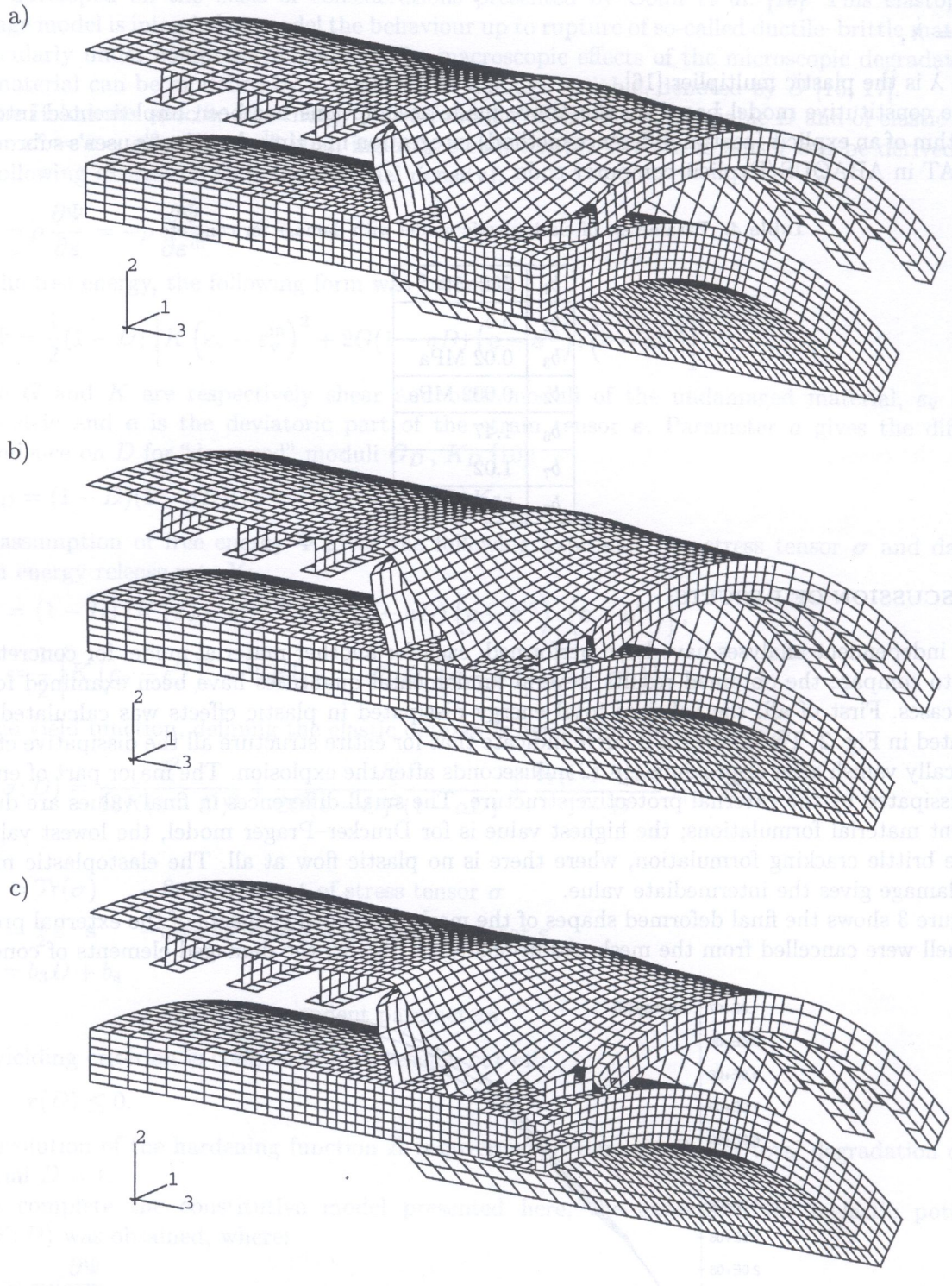

Fig. 3. Deformed mesh for various material models assumed for concrete: a) Drucker–Prager; b) brittle cracking; c) elasto-plastic model with damage

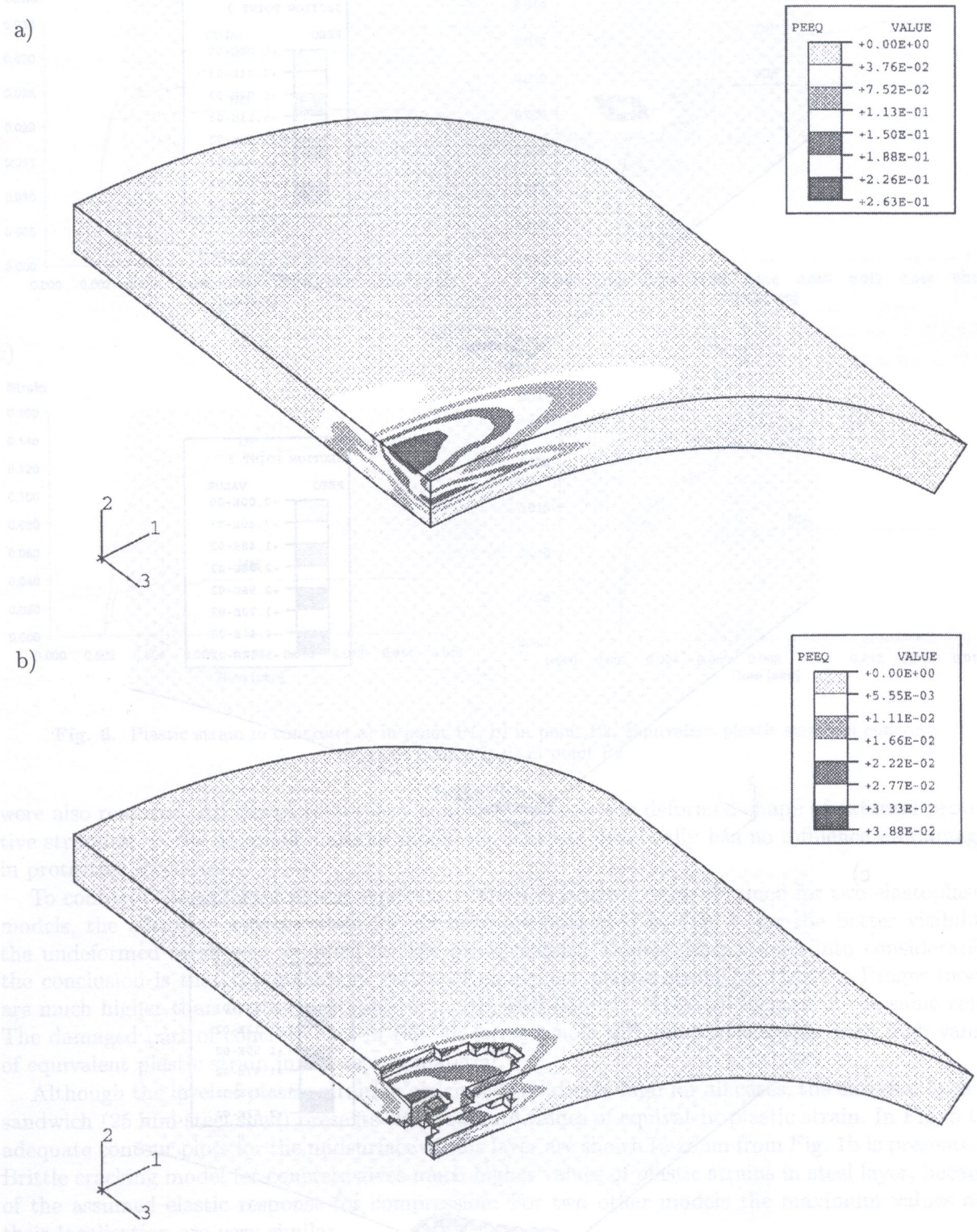

Fig. 4. Equivalent plastic strain in concrete layer for various material models: a) Drucker–Prager concrete model; b) elasto-plastic model with damage

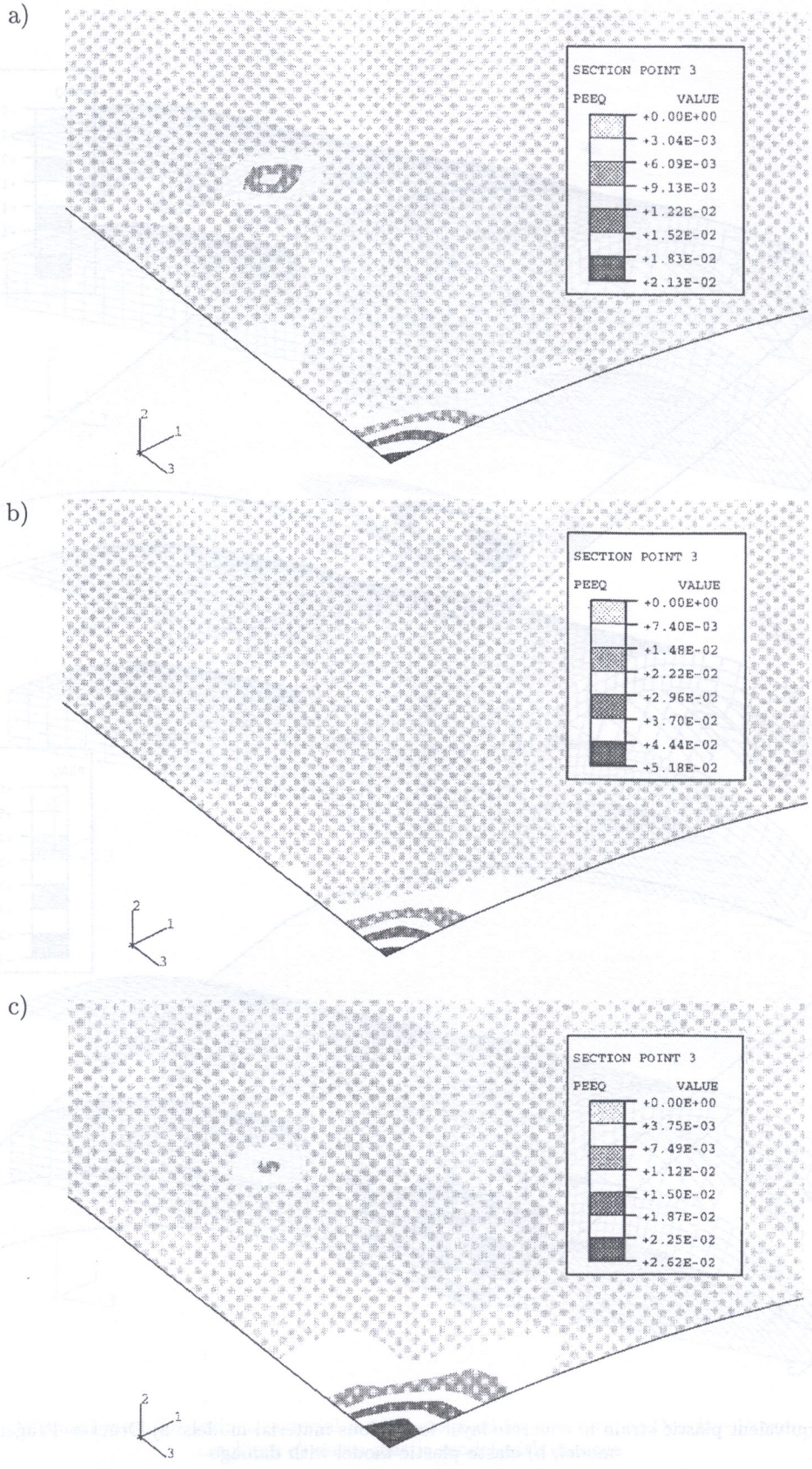

Fig. 5. Equivalent plastic strain in upper steel layer for various material models assumed for concrete: a) Drucker–Prager; b) brittle cracking; c) elasto-plastic model with damage

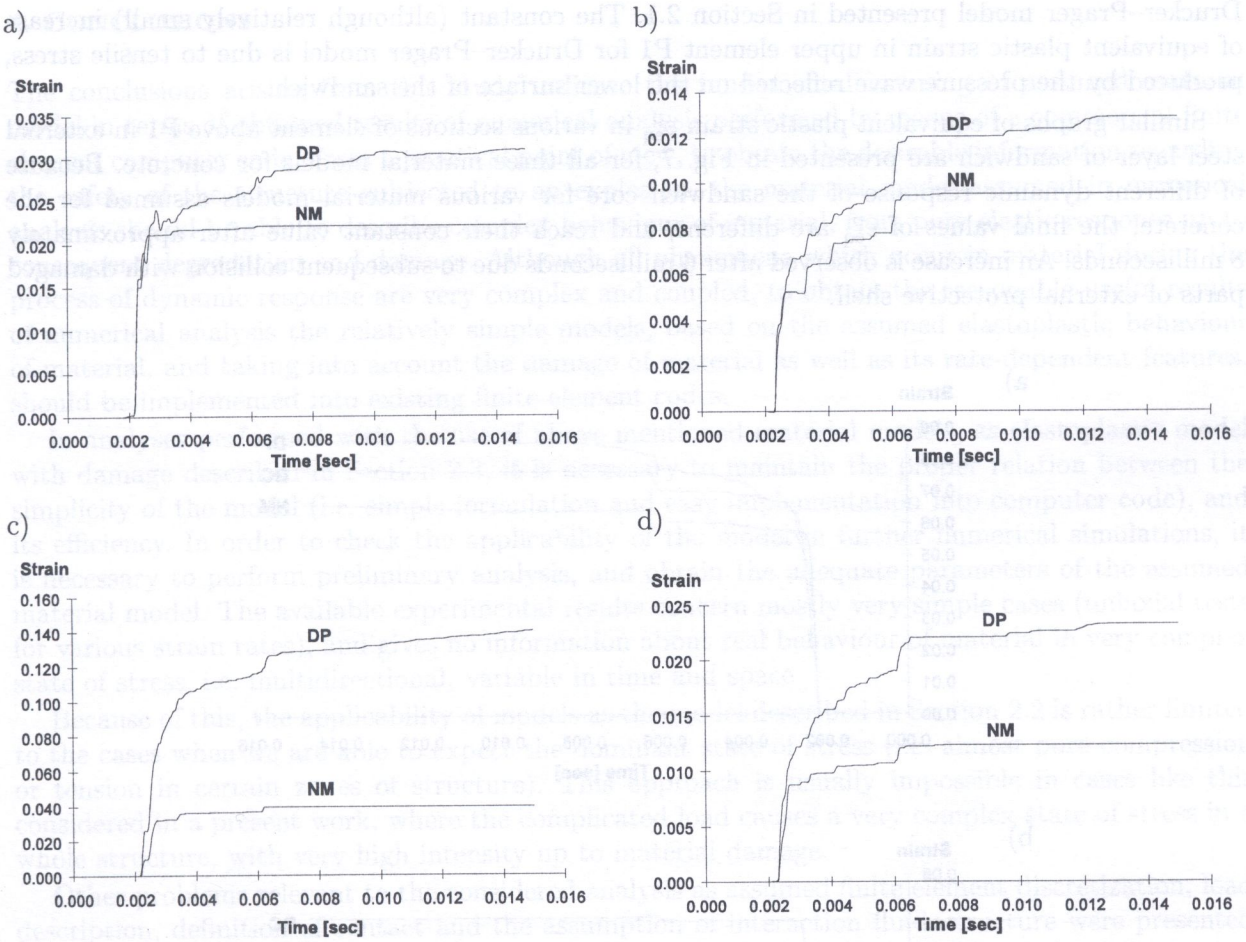

Fig. 6. Plastic strain in concrete: a) in point P1; b) in point P2. Equivalent plastic strain in concrete: c) in point P1; d) in point P2

were also removed. All the plots are very similar as regards the deformed shape of external protective structure — the assumed material model for concrete practically has no influence on damages in protective structure.

To compare the values of plastic equivalent strain in concrete core obtained for two elastoplastic models, the adequate contour plots for concrete are presented in Fig. 4 (for the better visibility, the undeformed mesh was assumed for the presentation). Taking those results into consideration the conclusion is that the maximum values of equivalent plastic strain for Drucker–Prager model are much higher than for the elastoplastic model with damage, although located in the same zone. The damaged part of concrete core in Fig. 4b forms a hole through its thickness, with high values of equivalent plastic strain in the rest of material.

Although the level of plastic strain in concrete is relatively high for all cases, the external layer of sandwich (25 mm steel shell) presents the moderate values of equivalent plastic strain. In Fig. 5 the adequate contour plots for the midsurface of this layer are shown (a zoom from Fig. 1b is presented). Brittle cracking model for concrete gives much higher values of plastic strains in steel layer, because of the assumed elastic response for compression. For two other models the maximum values and their localisation are very similar.

The results mentioned above regard the final state of the structure. To observe the development of plastic strain in time, the diagrams of plastic strain $\varepsilon_{22}^{\mathrm{p}}$ (global vertical direction) for elements P1 and P2 (Fig. 1b) and equivalent plastic strain $\varepsilon_{11}^{\mathrm{p}}$ versus time are presented in Fig. 6. Only the elastoplastic models are presented on the diagrams. For the elastoplastic model with damage, described in Section 2.3, the levels of plastic strain for both cases are considerable lower than for

Drucker–Prager model presented in Section 2.1. The constant (although relatively small) increase of equivalent plastic strain in upper element P1 for Drucker–Prager model is due to tensile stress, produced by the pressure wave reflected on the lower surface of the sandwich.

Similar graphs of equivalent plastic strain $\varepsilon^{\mathrm{P}}_{\mathrm{eq}}$ in various sections of element above P1 in external steel layer of sandwich are presented in Fig. 7, for all three material models for concrete. Because of different dynamic response of the sandwich core for various material models assumed for the concrete, the final values of $\varepsilon^{\mathrm{P}}_{\mathrm{eq}}$ are different, and reach their constant value after approximately 8 milliseconds. An increase is observed after 6 milliseconds due to subsequent collision with damaged parts of external protective shell.

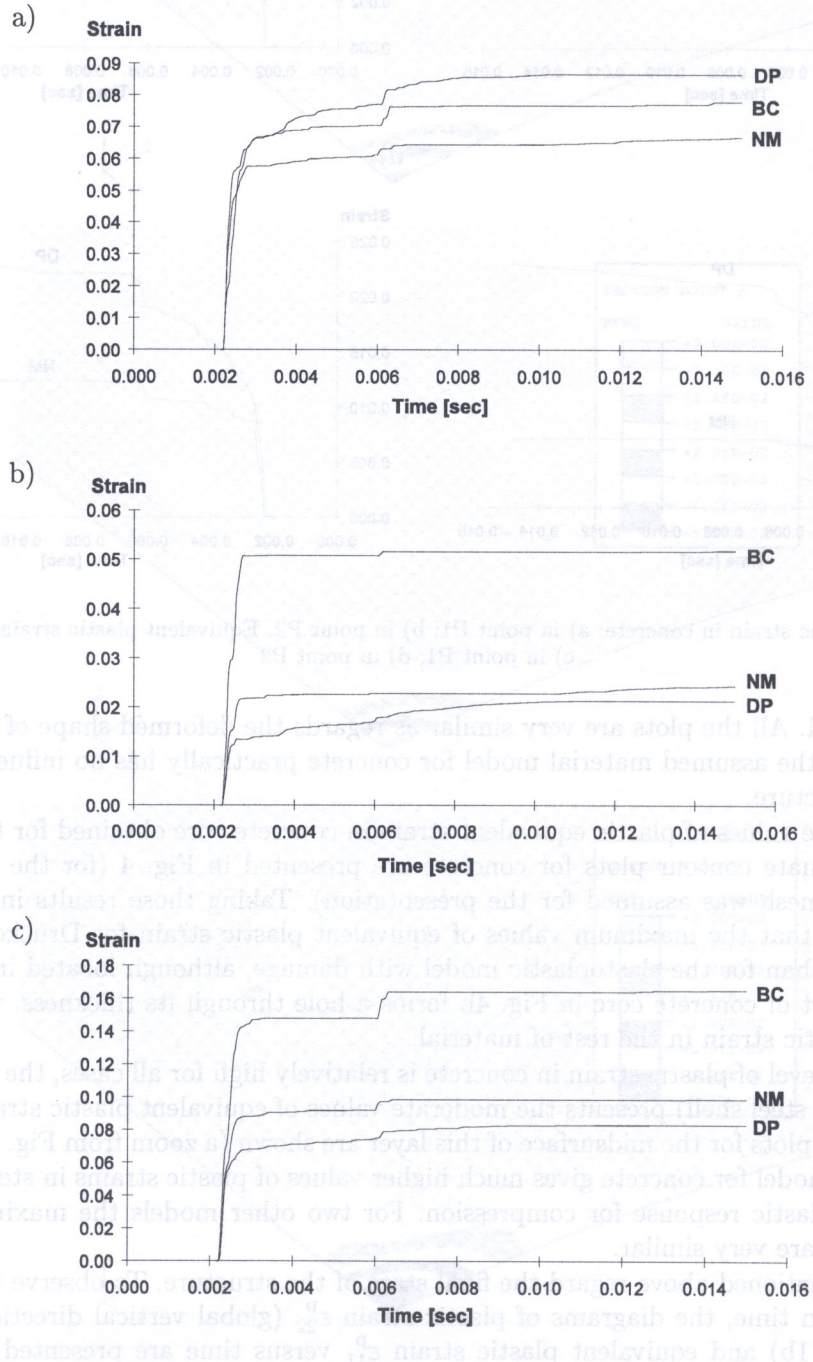

Fig. 7. Equivalent plastic strain in the corner element of upper steel versus time: a) botom surface, b) midle surface, c) top surface

4. Conclusions

The conclusions arising from this study indicate the fundamental meaning of assumed material model in terms of obtained results of numerical analysis performed by means of a commercial finite element computer code. From a practical point of view, to obtain the desirable information regarding the safety of the structure subjected to an explosion, the material model assumed in numerical analysis should be able to describe complex behaviour of material, from pure elastic response up to consequent degradation and damage. Although all phenomena which occur in material during the process of dynamic response are very complex and coupled, to obtain the reasonable useful results of numerical analysis the relatively simple models, based on the assumed elastoplastic behaviour of material, and taking into account the damage of material as well as its rate-dependent features, should be implemented into existing finite element codes.

In analyses performed with the use of above mentioned material models, as elastoplastic model with damage described in Section 2.3, it is necessary to maintain the proper relation between the simplicity of the model (i.e. simple formulation and easy implementation into computer code), and its efficiency. In order to check the applicability of the model in further numerical simulations, it is necessary to perform preliminary analysis, and obtain the adequate parameters of the assumed material model. The available experimental results concern mostly very simple cases (uniaxial tests for various strain rates), and gives no information about real behaviour of material in very complex state of stress, i.e. multidirectional, variable in time and space.

Because of this, the applicability of models as the model described in Section 2.2 is rather limited to the cases when we are able to expect the dominant state of stress (i.e. almost pure compression or tension in certain zones of structure). This approach is usually impossible in cases like this considered in a present work, where the complicated load causes a very complex state of stress in a whole structure, with very high intensity up to material damage.

Other problems relevant to the considered analysis as assumed finite element discretization, load description, definition of contact and the assumption of interaction fluid–structure were presented and discussed in papers [2, 6–9], but still present the source of doubts and questions. The further development of professional finite element computer codes intended for a numerical simulation of highly nonlinear phenomena, as the dynamic response of structures subjected to impulsive loading due to explosion should take into account the needs of such kind of analyses. The most salient necessity is the implementation of the efficient, simple defined, verified and reliably material models, provided for most common engineering materials.

Acknowledgements

The investigation was carried out under a research grant 7 T07E 060 08 of the Committee for Scientific Research (KBN). This support is gratefully acknowledged.

References

[1] *ABAQUS Theory Manual ver. 5.7.* Hibbitt, Karlsson & Sorensen, Pawtucket, USA, 1997.

[2] R. Adamczyk, K. Cichocki, M. Ruchwa. Analysis of the shock response of an underwater structure subjected to a far-field explosion. In: *Proceedings of ABAQUS Users' Conference, Milan, Italy*, Hibbitt, Karlsson & Sorensen, 1997.

[3] M.Y.H. Bangash. *Impact and Explosion – Analysis and Design.* Blackwell Scientific Publications, Cambridge, 1993.

[4] P.H. Bishoff, S.H. Perry. Impact behavior of plain concrete loaded in uniaxial compression. *Journal of Engineering Mechanics*, **121**: 685–693, 1995.

[5] W. Chen. *Constitutive Equations for Engineering Materials*, Vol. 2: *Plasticity and Modelling.* Elsevier, Amsterdam, 1994.

[6] K. Cichocki, R. Adamczyk, M. Ruchwa. Effect of protective coating on underwater structure subjected to an explosion. In: R. de Borst *et al.*, eds., *Proceedings of EURO-C International Conference "Computational modelling of concrete structures"*, 623–631, Balkema, Badgastein, Austria, 1998.

[7] K. Cichocki. Computer analysis of dynamic response due to underwater explosion on a hybrid structure. In: *Proceedings of ABAQUS Users' Conference, Newport, USA*, 207–220, Hibbitt, Karlsson & Sorensen, 1994.

[8] K. Cichocki, G. Maier, U. Perego. Analysis of damages due to underwater explosions on a hybrid structures. *International Journal for Engineering Analysis and Design*, **1**: 341–361, 1994.

[9] K. Cichocki, G. Maier, U. Perego. On numerical simulations of explosions on sealines. In: J. Najar, ed., *Proceedings of 9th DYMAT Technical Conference*, Munich, Germany, 1995.

[10] C. Comi, Y. Berthaud, R. Billardon. On localization in ductile–brittle materials under compressive loadings. *Eur. J. Mech. A/Solids*, **14**: 19–41, 1995.

[11] A.M. Rajendran, R.C. Batra (eds.). *Constitutive Laws. Experimental and Numerical Implementation.* CIMNE, Barcelona, Spain, 1995.

[12] J. Henrych. *The Dynamics of Explosions and Its Use.* Elsevier, Amsterdam, 1979.

[13] R.W. Hertzberg. *Deformation and Fracture Mechanics of Engineering Materials.* Wiley, New York, 1996.

[14] M.N. Islam, K. Kormi, S.T.S. Al-Hassani. Dynamic response of a thin-walled cylinder to side pressure pulse. *Eng. Struct*, **14**: 395–412, 1992,

[15] Y.W. Kwon, P.K. Fox. Underwater shock response of a cylinder subjected to a side-on explosion. *Computers and Structures*, **48**: 637–646, 1993.

[16] J. LeMaitre. *A Course on Damage Mechanics.* Springer-Verlag, Berlin, 1996.

[17] J. LeMaitre, J.L. Chaboche. *Mechanics of Solid Materials.* Cambridge University Press, 1990.

[18] T.C.K. Molyneaux, L.Y. Li, N. Firth. Numerical simulation of underwater explosion. *Computers Fluids*, **23**: 903–911, 1994,

[19] F. Salvatorelli. Dynamic response and failure of singular and sandwich cylindrical shells under lateral blast loading. In: P.S. Boulson, ed., *Structure under Shock and Impact*, 381–395, Elsevier, Amsterdam, 1989.

[20] R.S. Srivastava. *Interaction of Shock Waves.* Kluwer Academic Publishers, Dordrecht, 1994.

[21] D.C. Stouffer, L.T. Dame. *Inelastic Deformation of Metals.* Wiley, New York, 1996.

[22] J.W. Tedesco, C.A. Ross, P.B. McGill, B.P. O'Neil. Numerical analysis of high strain rate concrete direct tension tests. *Computers and Structures*, **40**: 313–327, 1991.

[23] J.W. Tedesco, M.L. Hughes, C.A. Ross. Numerical simulation of high strain rate concrete compression tests. *Computers and Structures*, **51**: 65–77, 1994.

[24] A.C. Singhal, D.S. Larson. Computer simulation of weapon blast pressures on flexible surfaces. *Computers and Structures*, **41**: 325–330, 1991.